2015 28th International Conference on VLSI Design and 2015 14th International Conference on Embedded Systems

NFC For Pervasive Healthcare Monitoring

Prabhakar T V, Ujwal Mysore
Department of Electronic Systems Engineering
Indian Institute of Science,
Bangalore,India-560012
Email: (tvprabs,ujwal.s)@dese.iisc.ernet.in

Uday Saini, Vinoy K J and Bharadwaj Amruthur
Department of Electrical Communication Engineering
Indian Institute of Science,
Bangalore,India-560012
Email: uday.s.saini@gmail.com,(kjvinoy,amrutur)@ece.iisc.ernet.in

***Abstract*—We undertake a step-by-step approach in the design of two Near Field Communication (NFC) products for pervasive healthcare monitoring. Our first product is an NFC based battery charger circuit to charge a thermometer equipped with wireless communication. Our system design has a simple linear charger, with overvoltage and undervoltage protection implemented as an android App. The NFC power source provides $13-15$ mW of continuous power and is able to charge a 45mAH battery in about 10 hours from deep discharge to full charge state. Since the weight of the charger is about 3 grams and the size is about 2 cms in diameter, this product is useful for wearable sensor devices and provides a convenient way of recharging the batteries without the need for any connectors in the device. This allows devices to be hermetically sealed, besides enabling smaller form factors. The second product is an NFC based battery-less medical grade thermometer. To obtain the temperature of a single patient, a maximum of 10 seconds is sufficient to read the sensor value starting from placement of a smartphone over the product.**

I. Introduction

Similar to Radio Frequency Identification (RFID), Near Field Communication (NFC) is capable of battery-less powering and data backscatter communication. At the same time, there are also some key differences between them such as NFC's interchangeable roles of Interrogator and Transponder. NFC can achive data rates upto 424 kbps. While the standard specifies a range of about 22 cms, in practice the range does not exceed about $1-3$ cm, this make data communication more secure. Depending on the application, NFC has three modes of operation as follows:- (a) Card emulation mode (b) Peer to Peer mode (c) Read/Write mode. Some examples of card emulation mode are payment for goods and services, boarding a public transport system such as bus and metro rail. Some examples of peer to peer is transfer of an image from one NFC enabled device to another one. An example of Read/Write mode includes printing from a camera and retrieving information by touching a poster in museums and public places etc. Since NFC is based on inductive wireless power transfer, it is an attractive energy harvesting option due to its high efficiencies. Furthermore, being contactless with significant penetration in smartphones, improves its usability and finds applications in healthcare; as infection prevention is automatically taken care. In one early application of NFC for public healthcare, the work by Massachusetts Institute of Technology proposed its use as a wearable on patients visiting a hospital for pneumonia detection [1]. In the event of an affirmative detection, the surveillance and monitoring of quarantined patients is greatly aided by an NFC enabled phone. This application is restricted to perform the role of a tracking device. Since the current gap in literature is its application as part of a health care device, our goal is to demonstrate NFC's capability to address this gap.

Our design philosophy is a wearable device for patients to facilitate uninterrupted and continuous monitoring of body temperature in a hospital setting or home under the supervision of care givers. To this end, we build from scratch two compelling light weight products centred around an android smartphone: (a) An NFC battery charger for a medical grade Bluetooth Low Energy based thermometer (b) A battery-less NFC enabled medical grade thermometer for intermittent but regimentation based monitoring. These can also be used to continously monitor temperature of neonates with low birth weight.The first four weeks of child birth are critical for such neonates, continous monitoring of critical parameters , such as temperature are important [2]. This is due to the fact that such babies have the inability to retain their body heat, resulting in hypothermia. Hypothermia in patients can be fatal within 30 minutes of its onset. Thus, this baby friendly device has the requirement that calls for a battery based, lightweight device with continuous power. However, charging such devices can be cumbersome, particularly if the device is a sealed package. On the other hand, the NFC based thermometer is expected to be used beyond the 4 week period where temperature monitoring is important, but not particularly continuous. The NFC modes for these two products cover both card emulation and read/write mode. Also, since medical data is only a few bytes, low data rates and secure communication are attributes to select NFC as a perfect candidate. We think that our step by step approach in system design is generic enough to build several other products.

II. Literature Survey

The work by Johan et al, installs an NFC system interleaved within the bandage to sense the dryness of wounds [3]. Change in resistance method is used for detection of bleeding. Another application is detection of urine in elderly persons by placing the NFC system within diapers worn by them. The analog value is read by the system and stored in available memory within the NFC chip. In our work, we have an NFC system with an ultra low power microcontroller for the purposes of intelligence and computation. Since our NFC application is a thermometer module, it is non-invasive and thus reduces the risks of infection. The work by Hillukkula et al, conduct an extensive study related to RF field generation by several commercial NFC readers [4]. Furthermore, they perform detailed power budget calculations. They show that, due to timing constraints, UART communication is non trivial between NFC and a microcontroller. In our work, we address

1063-9667/15 $31.00 © 2015 IEEE
DOI 10.1109/VLSID.2015.18

this issue elegantly. We exploit the delay available between the NFC powering mode and tag detection mode. In the two products we previously mentioned, efficient power generation and its management is the key. At the same time, size, weight and patient friendliness of the product is important.

III. System Design

Inductive charging uses an electromagnetic field to transfer energy between two objects. In RF engineering parlance, this is called Wireless Power Transfer (WPT). The nature of this transfer is non-radiative. Inductive charging via magnetic coupling of coils is one such method that is utilized in this work. The concept behind this setup is also called Transformer Action, as the primary and secondary sides of the circuit are not electrically connected, with the primary side delivering power and the secondary side containing the load. Our work deploys the concept of Inductive Power Transfer (IPT) at a frequency of 13.56MHz (ISM Band).

A. Inductive charging - conceptual outline:

An IPT scheme utilizes a primary coil with an excitation of a suitable frequency, and a secondary coil that must be placed within the region of magnetic flux generated by the primary coil for an Electromotive force (emf) to be induced in the secondary coil. The value of this induced emf depends on two factors. Firstly, the coupling coefficient, which is effectively a measure of the percentage of flux generated by the primary coil incident on the secondary coil. Second, the value of self-inductance of the secondary coil. As the hand-held devices technology advances, smartphones are becoming more pervasive and ubiquitous. A smartphone acts as a power source by using its NFC module to beam some power in an attempt to pair up with other NFC capable devices in its immediate vicinity. IPT in our application is dedicated towards charging a battery (Standard 3V Li-ion rechargeable coin cell with a diameter of approximately 20mm), thus our secondary side must be within a comparable dimensional footprint. The use of 13.56 MHz as our frequency of operation as opposed to lower frequency ranges in commercial IPT standards such as Qi, assists in lowering the required inductance value and hence decreasing the feature size.

B. Harvester Design:

To utilize an NFC capable Phone/transmitter and harvest energy from it, we need, at the receiver side, a passive NFC tag. AS3953 NFC IC fits our requirements, as it offers a user-configurable external voltage that can be extracted from the incident magnetic field, offers an internal resonance capacitor in order to improve the efficiency of harvesting [5]. This tag connects to an external coil that acts as an antenna for receiving power. The coil is connected to the internal resonant capacitor whose value is within a range of 27-35pF to increase the efficiency of energy harvesting [5]. Given this range of resonant capacitance values, the resulting inductance value for the coil should be between 3.9-5.1μH so as to enable the harvesting circuit to operate near resonance point. Thus we now have the following specifications related for the coil design: Firstly, Maximum Outer diameter lesser than 19mm. Secondly, Self-Resonant Frequency much greater than 13.56 MHz. Lastly, Maximum and Minimum inductance values for efficient operation are 5.1μH and 3.9μH. The coil must be on a printed circuit board so as to directly connect to our AS3953 NFC tag, which has 2 pins allocated for the coil input.

1) Coil Design: Efficiency in an IPT system is largely affected by good coupling between the primary and secondary coils. Furthermore, coupling between two coils depends on their respective self-inductance, Quality Factor, and a high Mutual Inductance between the coils. Given the dynamics posed by constraints for our application, the parameters for the coil used on the primary side (inside the Smartphone) is outside the design scope, thereby pushing all the design challenges to the coil on the secondary side. In principle, an IPT link would appear as shown in the Figure1.

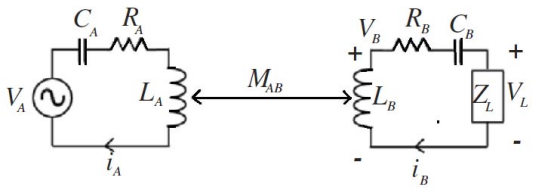

Fig. 1. Inductive Power Transfer

The mathematical description for such a link is [6]

$$V_A = j\omega L_A i_A + i_A/j\omega C_A + R_A i_A - j\omega M_{AB} i_B \quad (1)$$

$$j\omega M_{AB} i_A = j\omega L_B i_B + i_B/j\omega C_B + R_B i_B + Z_L i_B \quad (2)$$

Exact quantitative behaviour may differ with implementations. It becomes clear that for a higher induced voltage in the secondary coil, M_{AB}, should be as high as possible.

$$M = K\sqrt{(L_1 L_2)}. \quad (3)$$

where M is the mutual inductance between two coils having a self-inductance of L_1 and L_2 respectively and K is the coefficient of coupling which varies from 0 to 1. This in physical terms is a ratio of the flux passing through the secondary to the flux generated by the primary. Thus to increase M, we have three controllable parameters, namely L_1, L_2 and K. In our case, since L_1 is fixed, we can modify L_2, the secondary inductance and K, the coupling coefficient. Given the nature of IPT, we cannot expect a K equal to 1, due to a separation between the two sides. Therefore, me must try to maximize the value of K and use a large value inductance. However, the value of inductance cannot exceed a certain limit due to physical and electrical constraints. Thus we need to design a small sized high inductance. One way to describe the efficiency of an inductive link is as [7]

$$\eta = \frac{(K^2 Q_1 Q_2)}{(1 + \sqrt{(1 + K^2 Q_1 Q_2)})^2} \quad (4)$$

Where K is the coupling coefficient and Q_1 and Q_2 are the quality factors of primary and secondary coils respectively. For coil design, our primary goal is to maximize K (as we are bound to some extent with the values of inductance desired and the size), and reduce its dependency on spatial orientation w.r.t. the primary coil. Thus our secondary coil must ensure sufficient Q and a high inductance and should focus on getting a high value of K when coupled with the primary coil, which is usually a spiral coil housed inside the smartphone. Printed spiral coils in either circular or polygonal shape can be easily and cheaply manufactured and are widely used in RF applications. A Printed spiral coil is chosen for our application as it helps in achieving a high coupling coefficient and provides robustness to the design by lowering misalignment sensitivity [8].

2) Coil inductance calculations: A square spiral coil is the most popular choice in the designing of coils in RFID. However at times, designers use polygonal or circular coils to improve performance. In our case, since the goal is to deliver power wirelessly to chargeable coin cell Li-ion battery, it is best to utilize this area by using a circular coil as the battery itself of 20 mm diameter. For comparison and demonstration purposes we have also shown a square coil.

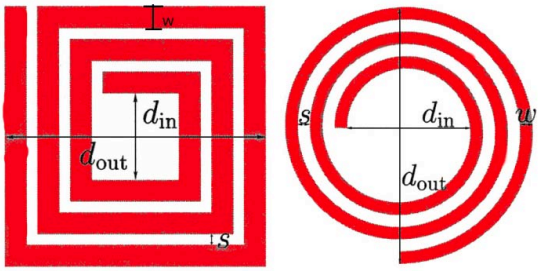

Fig. 2. Coils with different Geometry

For single layer spiral inductors from figure 2 is given by [9]:

$$L = \frac{(\mu_0 n^2 d_{avg} c_1)}{2(ln\frac{c_2}{\varphi} + c_3\varphi + c_4\varphi^2)} \tag{5}$$

Where φ is called the fill factor, and is equal to $\frac{(D_0 - D_i)}{(D_0 + D_i)}$. The constants Ci's depend on the layout geometry. d_a is the average diameter, $\frac{(Do+Di)}{2}$. D_0 and D_i are the outermost and innermost diameters of the coil. N is the number of turns in the coil. And $\mu_0 = 4\pi \times 10^{-7} H/m$. is the magnetic permeability of free space. Table I shown below has constant value for different geometric shapes.

TABLE I. CI CONSTANTS FOR DIFFERENT GEOMETRY

Layout	C1	C2	C3	C4
Square	1.27	2.07	0.18	0.13
Circular	1.0	2.46	0.0	0.2

The above Equation [5] is based on current sheet approximation of the sides of spiral by symmetrical current sheets of equivalent current densities Equation [5] is also called Greenhouse Formula [10][11]. In addition to this, there are several other closed form equations to approximate the inductance for printed spiral coils that are also cited in a few other related works[12],[13],[14]. A few other factors that influence the inductance are number of layers, metal spacing and conductor width are discussed in [15]. In addition to these, there is another suitable closed form expression given by wheelers in [16]

$$L = \frac{(31.33\mu_0 N^2 a^2)}{(8a + 11c)} \tag{6}$$

Here N is the number of turns, 'a' is the average radius $\frac{(R_0+R_i)}{2}$, and 'c' is the radial thickness $\frac{(R_0-R_i)}{2}$. And $\mu_0 = 4\pi \times 10^{-7} H/m$. is the magnetic permeability of free space.

3) Simulation Results: With a targeted range of the required coil inductance specified, equations [5]for circular geometry and [6] were used to arrive at the design specifications of the coil as shown in Table II.

TABLE II. DESIGN SPECIFICATION OF THE COIL

Parameter	Value
Area(A)	$222mm^2$ (approx.)
Inner Radius(Ri)	3.5mm
Outer Radius(Ro)	8.3mm
Number of turns(N)	19
Conductor Width(w)	0.128mm
Conductor Spacing(s)	0.128mm
Number of layers	1
Self-Resonant Frequency	28.5MHZ
Inductance(uH)	4.9μH (Theoretical), 4.5μH (simulated)
Inductance Density	22nH/mm^2 (Theoretical) 20.2nH/mm^2(simulated)
Copper Thickness	35μm

A square coil with the same inner and outer diameters (also φ) as our circular spiral coil has a calculated inductance of 5.8μH and an area of 275mm^2 ,which results in a theoretical inductance density of 21nH/mm^2, but the maximum feature size of a square with same Do as the circular coil has a diagonal that is larger($\sqrt{(2D_0)}$) than the maximum feature size desired. A square spiral coil that fits inside our target area must have a diagonal that equals the outer diameter of our current circular coil, therefore its side length must be equal to 11.7 mm. With a minimum possible pitch of .256mm per turn due to manufacturing constraints the resulting maximum inductance was in the range of 2.2-2.8μH equation[5], with various design parameters tweaked. The variation of 8% between simulated and predicted value of the inductance can be attributed to presence of copper pads in the layer of circuit below the coil which results in an increase in the fill factor, which can cause a drop in the inductance. Further, variations less than 20% have been reported in literature [17]. Figure 3 explains the simulation results of the designed coil.

IV. NFC BATTERY CHARGER

Figure 4 shows the top and bottom view of the charger circuit respectively. The battery recharging module consists

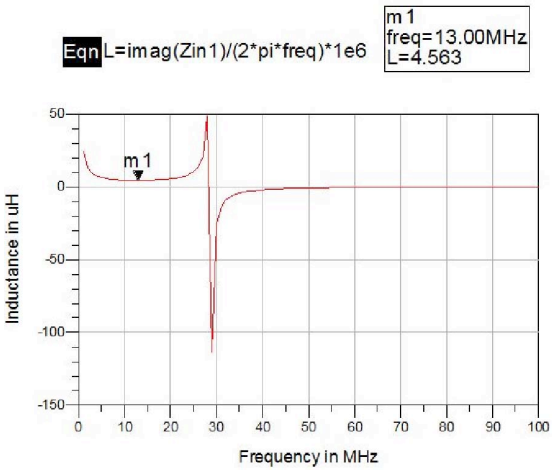

Fig. 3. Simulation Results

Fig. 4. Coil with charger circuit

of a 19mm diameter 0.8mm thick substrate coil antenna. We used an NFC interface chip AS3953A that can harvest the energy from an NFC enabled android smartphone that provides an output voltage of 3.3 volts and delivers maximum output current of 5mA. Figure 5 shows a simple linear charging circuit to recharge a Li-ion battery. Table III shows the battery charging parameters for two different smartphones. Since the energy harvested by this system is best determined using a capacitor, Table IV shows the charging parameter to store energy in a 15mF supercapacitor. It is observed that Sony phones can provide a higher power output and range compared to Google Nexus phones, perhaps due to a higher mutual inductance. The energy generated by the Nexus is about 75uJ in 21 seconds as compared to 73.3uJ generated in 13 seconds by Sony phone. Also, their operating range is about 1.5 cm and 0.5 cm respectively.

TABLE III. BATTERY CHARGING PARAMETERS

smartphone	Sony Experia SP	Nexus 5
Harvested Voltage(V)	3.34	3.3
No Load Current(mA)	4.98	4.0
Battery Voltage before charging(V)	2.61	2.56
Charging Current(mA)	2.7	2.2

4) Soft PMIC: A Power Management IC(PMIC) may include battery management, voltage regulation, and charging functions. It may include a DC to DC converter to allow dynamic voltage scaling[18][19]. Battery management includes a battery charger which is used to pump energy into a secondary cell or rechargeable battery without hampering the storage capacities [20]. Generally Li+ batteries work in

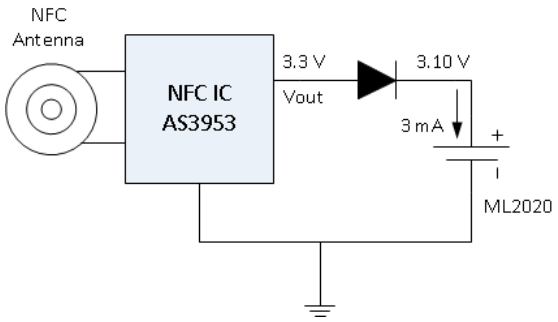

Fig. 5. Linear Battery Charging Unit

TABLE IV. CHARGING PARAMETERS FOR A SUPERCAPACITOR

smartphone	Sony Experia SP	Nexus 5
Initial capacitor Voltage(V)	0.13	0.02
Start time (s)	0	0
Final capacitor Voltage(V)	3.13	3.2
End Time(s)	13	21
Charging Current(mA)	3.5	2.3

the range of 1.8- 3.3 volts are charged either in constant current or constant voltage method. Li+ batteries offer good charging performance at cooler temperatures and may even allow ”fast-charging” within a temperature range of 5 to 45 deg C (41 to 113 deg F). We selected ML2020 super compact lithium secondary batteries which are rated for 45mAH at 3V. Manganese compound oxide is used for the positive electrode, and a Lithium/aluminium alloy for the other electrode. It is sufficient to charge these batteries with C/15 charge at 3mA. Hence, charging time for mentioned battery capacity is about 12- 15 hours from its deep discharge state i.e., 1.8V. However, the charging circuit that we used [Figure 5] , recommends to recharge the battery when its terminal voltage falls to 2.5 Volts to avoid deep discharge.We can recharge the battery by enabling the NFC in smartphone and placing the harvester in close proximity. We envisage that the system is left in pairing mode overnight; for a specified duration of 10 hours. In our case, since there is no power management IC, we exploit the power management by way of a smart android Java based application. From fig 5 we observe that the circuit is limited to charging a battery but has zero intelligence related to power management and safety. Generally power management IC’s are capable of functions such as undervoltage protection, overvoltage protection, boost and buck conversion. In this work, we implement most of these functions in software. To demonstrate our idea, we connected the battery terminals to the input of analog to digital port to sense its voltage. Figure 7 support this functionality(circuit diagram is not shown but similar to Figure7). In the existing system, the buck and boost conversion is replaced by the harvested regulated output by NFC chip. NFC chip is capable of providing an output voltage at three different levels which are 1.8, 2.7 and 3.3 volts. In general, rechargeable batteries are at 3.3v and hence the current system is configured to provide this constant voltage. This section explains electrical safety related to battery which is carried out entirely in software i.e., power management is achieved in NFC enabled android smartphone. When the battery reaches the under voltage condition, a green colored

LED will glow; prompting the user to recharge the battery. When the smartphone is brought near this module, the whole system is powered and battery voltage is sensed continuously and updated in the EEPROM of the NFC chip. This data is read by the smartphone and as soon as the specified voltage is achieved, a prompt is sent to the the user to disable the NFC on the smartphone. Since android has limitations of automatically turning off NFC, we prompt the user to manually turn off the NFC on the smartphone. Here we have android app, (amsNFC) from Austria micro systems. This application is modified to read the voltage level of the battery from EEPROM of NFC chip and prompt the user to use NFC accordingly. Figure 6 is the screenshot of modified app prompting the user to turn off the NFC in smartphone.

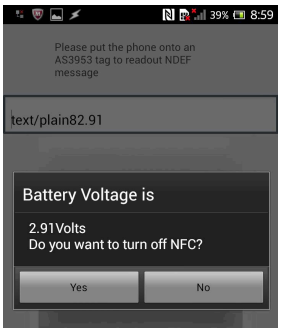

Fig. 6. Screenshot of the app where we are prompting user to turn off the NFC

V. NFC Battery-less Thermometer

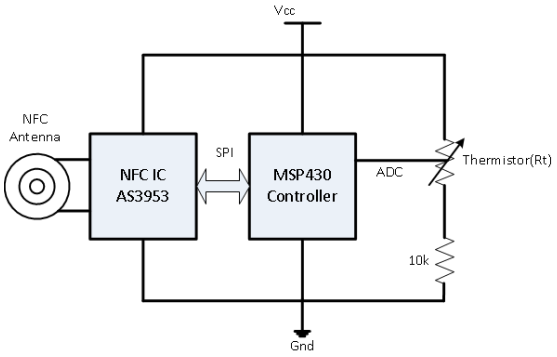

Fig. 7. System Block Diagram of Battery-less Thermometer

Figure 8 shows the physical size of the battery-less thermometer. It consists of a low power microcontroller MSP430F2132, a medical grade thermistor from Cantherm, an NFC chip from AMS and an accompanying 19 mm diameter coil antenna. The NFC chip has an internal 1Kbit EEPROM. It is also configured to follow NFC Standard ISO 14443A level 4 protocol. The protocol standard specifies that NFC chip EEPROM accessibility over reader field is preferred compared to SPI access.

Figure 9 describes how we can exploit the ISO14443A type 4 protocol to access EEPROM in tag detection mode. The Vout represents the output voltage from the NFC enabled android phone. Since NFC provides pulsed power, The NFC reader

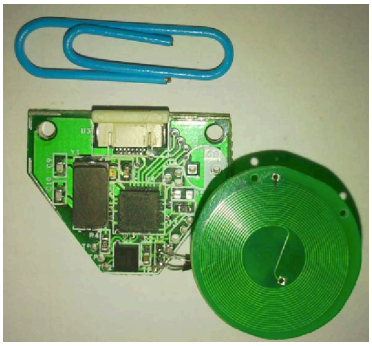

Fig. 8. Thermometer with the harvester

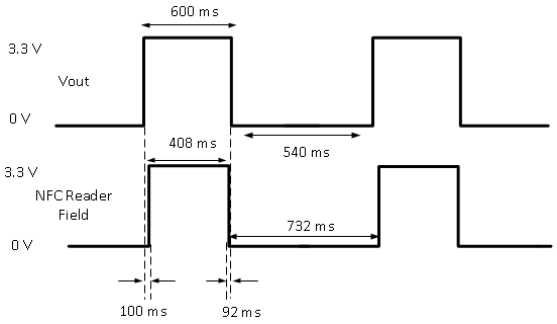

Fig. 9. Power harvested under reader field

(Android phone) will detect the NFC tag 100ms after the NFC IC powers up and detection ends 92ms before power down. The figure explains the exploitation of the EEPROM access over SPI before and after NFC reader field in tag detection mode. Hence, NFC memory can be accessed by controller and also the reader restricted to this window. The thermistor MF51E103 has a resistance value of 10K Ohm at 25 deg C and used for measuring the temperature.

$$\frac{1}{T} = A + Bln(R_T) + C(ln(R_T))^3 \quad (7)$$

The temperature-resistance characteristics of the thermistor is given by the polynomial Steinhart-Hart equation 7 where A,B and C are Steinhart-Hart coefficients. We used a 12 bit ADC and internal reference voltage of 2.5volts and the read ADC value is converted into corresponding temperature by using Equation 7.

As patient data requires secure transmission, data encryption is achieved on this module. Since key generation is an energy expensive operation, we move this function into the smartphone. At the same time, we provide the flexibility to change keys periodically, particularly when the module is passed on from one patient to another. We modified the NFC app to support this option and generated a 128 bit AES key with patient name as the seed to the Pseudo Random Number Generator. The generated key is then pushed into the NFC chip of the thermometer module. We explored two methods of key storage and its usage. Firstly, when the system is turned on, the microcontroller checks the NFC read flag condition on its flash. If the flag is set, it will then read the 128 bit key from NFC chip, store the key into flash of microcontroller

and clears the read flag. The flag is usually set during a factory programming. The key stored in the controller's flash is used for encrypting the patient data. In this mode, flash erase operation is performed for every key change on the module. In the second method, when the system is turned on, the microcontroller reads the key from NFC chip memory and does a write lock operation to the EEPROM of NFC chip. This write lock word prevents over-writing of the key by any other smartphone. This key lock method mode can support a finite number of reconfiguration attempts, due to limited by memory (1Kb) available in the NFC EEPROM. In our system, this number is three.

Table V shows the energy measurements for individual functions carried out by the system. The energy requirements is about 1mJ for these operations, significantly lower than energy generated by the system. When an NFC enabled smartphone is brought near this module, the NFC chip will power the entire module and read the ADC value. This value is converted into corresponding temperature by using equation 7, and writes the value into EEPROM of NFC chip. It is then communicated and displayed on the user smartphone. Figure 10 shows the screenshot of mobile app which displays the body temperature in degree centigrade.

TABLE V. ENERGY BUDGETING

Function	Energy Consumed(mJ)
ADC Sensing	0.97
Temperature Calculation	0.13
EEPROM write(4 bytes)	0.1

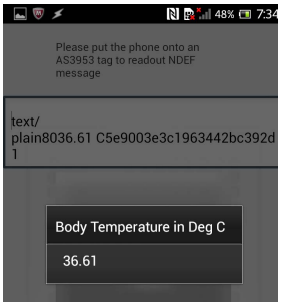

Fig. 10. Screenshot of the app displaying body temperature the NFC

VI. SUMMARY AND CONCLUSIONS

In this paper we have shown that NFC is a potential technology for healthcare products both for critical care continuous monitoring and regimentation based parameter monitoring. We have shown that encryption key reconfiguration has elegant solutions. These two novel products open up several possibilities to use battery-less as well as battery charging technologies from NFC enabled smartphone's reader field. This includes reconfiguration of devices, battery charging, configuration, sensing and other low power and low computational operations.

ACKNOWLEDGEMENT

The authors would like to thank the Robert Bosch Centre For Cyber Physical Systems, Indian Institute of Science, Bangalore, India for supporting this work.

REFERENCES

[1] A Marcus, G Davidzon, D Law, N Verma, R Fletcher, A Khan, L Sarmenta *Using NFC-enabled Mobile Phones for Public Health in Developing Countries* IRD 2009.

[2] *http://www.medicalhome.org/4Download/cec/elbw.pdf* date of visit- March 2013

[3] Johan Sidacn, V Skerved, J Gao, S Forsstram, H Nilsson, T Kanter, M Gulliksson *Home Care with NFC Sensors and a smartphone* ACM Proceeding ISABEL '11 Article No. 150

[4] Hillukkala Mika, H Mikko, Y Arto, *Practical implementations of passive and semi-passive NFC enabled sensors*First International Workshop on Near Field Communication,2009

[5] *www.ams.com* date of visit- Janury 2014

[6] Wei Chen, Sibrecht Bouwstra, Sidarto Bambang Oetomo and Loe Feijs *Intelligent Design for Neonatal Monitoring with Wearable Sensors, Intelligent and Biosensors* Vernon S. Somerset (Ed.), ISBN: 978-953-7619-58-9,2010.

[7] M. AhsanulAdeeb,*A Class E Inductive Powering Link with Backward Data Communication for Implantable Sensor Systems* Ph.D. Thesis, The University of Tennessee, Knoxville, 2006.

[8] C. M. Zierhofer and E. S. Hochmair, *Geometric approach for coupling enhancement of magnetically coupled coils*,IEEE Trans. Biomed. Eng., vol. 43, no. 7, pp. 708714, Jul. 1996.

[9] S. S. Mohan, M. M. Hershenson, S. P. Boyd and T. H. Lee, *S*imple Accurate Expressions for Planar Spiral Inductances,IEEE Journal of Solid-State Circuits, Vol. 34, No. 10, 1999, pp. 1419-1424. doi:10.1109/4.792620

[10] E. B. Rosa*Calculation of the self-inductances of single-layer coils* Bull. Bureau Standards, vol. 2, no. 2, pp. 161187, 1906.

[11] H. Greenhouse,*Design of Planar Rectangular Microelectronic Inductors*, IEEE Transactions on Parts, Hybrids, and Packaging, Vol. 10, No. 2, 1974, pp. 101-109. doi:10.1109/TPHP.1974.1134841

[12] F. W. Grover, *Inductance Calculations: Working Formulas and Tables.*New York: Van Nostrand, 1946.

[13] A. Balakrishnan, W. D. Palmer, W. T. Joines, and T. G. Wilson, *The inductance of planar structures*, in Proc.8th Annu. Appl. Power Electron. Conf. Expo., Mar. 711, 1993, pp. 912921.

[14] U Jow, M Ghovanloo *Design and optimization of printed spiral coils for efficient transcutaneous inductive power transmission.*IEEE Transactions on Biomed Circuits and Systems. 2007 Sep;1(3):193202.

[15] Islam Ashraf B; Islam Syed K; and Tulip Fahmida S *Design and Optimization of Printed Circuit Board Inductors for Wireless Power Transfer System*, 2013.

[16] THOMPSON:*Inductance Calculation Techniques — Part II: Approximations and Handbook methods Power Control and Intelligent Motion*,December 1999

[17] Daly D A, Knight S P, C Martin, Ekholdt R *Lumped Elements in Microwave Integrated Circuits," Microwave Theory and Techniques,*IEEE Transactions on , vol.15, no.12, pp.713,721,December1967 doi:10.1109/TMTT.1967.1126571

[18] *http://www.ti.com/lit/an/slyt451/slyt451.pdf* date of visit- June 2014

[19] *http://www.linear.com/products/powermanagement* date of visit- June 2014

[20] *http://www.collinsdictionary.com/dictionary/english/recharger* date of visit- June 2014